A comparison of the increased temperature accelerated degradation of Poly(d,l-lactide-co-glycolide) and Poly(l-lactide-co-glycolide)

Geddes, L., Carson, L., Themistou, E., & Buchanan, F. (2020). A comparison of the increased temperature accelerated degradation of Poly(d,l-lactide-co-glycolide) and Poly(l-lactide-co-glycolide). *Polymer Testing*, *91*, Article 106853. https://doi.org/10.1016/j.polymertesting.2020.106853

Published in:
Polymer Testing

Document Version:
Peer reviewed version

Queen's University Belfast - Research Portal:
Link to publication record in Queen's University Belfast Research Portal

A Comparison of the Increased Temperature Accelerated Degradation of Poly(*D,L*-lactide-*co*-glycolide) and Poly(*L*-lactide-*co*-glycolide)

L. Geddes[1], L. Carson[2], E. Themistou[3], F. Buchanan[1]

[1]School of Mechanical and Aerospace Engineering, [2]School of Pharmacy, [3]School of Chemistry and Chemical Engineering, Queens University Belfast, Belfast, Northern Ireland, UK

Abstract

Bioresorbable polymers composed of poly(lactide), poly(glycolide) and their related copolymers have become increasingly popular for the preparation of bone substitute constructs. *In vitro* tests assessing the degradative changes in physicochemical, mechanical, and biological properties of bioresorbable polymers are generally carried out at 37°C, in pH 7.4 phosphate-buffered saline (PBS). However, long degradation times, varying from months to years make it difficult to assess these polymers at their late stages of degradation. An increased temperature accelerated degradation methodology, that simulates the long-term degradation of poly(*D,L*-lactide-*co*-glycolide) and poly(*L*-lactide-*co*-glycolide), has been validated in this study. Samples were degraded in PBS, under sterile conditions. Degradation temperatures of 47°C, 57°C and 70°C were selected and compared to physiological temperature, 37°C. At predetermined time intervals, samples were retrieved and evaluated for changes in mass, swelling, molecular weight, crystallinity, and thermal properties. The results from this study suggest that the degradation mechanism at elevated temperatures is similar to that observed at 37°C. It is recommended that 47°C is adopted by the research community to accelerate the degradation of these polymers. It is hoped the application of this methodology could be used as a valuable tool, prior to the assessment of the long-term biocompatibility of these polymers.

Keywords

Poly(lactide-*co*-glycolide), bioresorbable, polymer, degradation, accelerated, molecular weight

1. Introduction

Traditionally, permanent metallic materials have been used in orthopaedic applications due to their high strength and inert nature. However, problems, such as stress shielding, implant migration or loosening and the risks associated with revision surgery have led to the development of implants based on bioresorbable polymers[1]. Upon *in vivo* implantation these polymers degrade *via* hydrolytic chain scission, as injured tissue regenerates, and are excreted from the body *via* metabolic pathways. Members of the poly(*α*-hydroxy acid) family such as polyglycolide (PGA), polylactide (PLA) and their related copolymers have been used in various biomedical applications including internal sutures, orthopaedic screws and scaffolds, drug delivery and tissue engineering[2]. PLA exists in two enantiomeric forms, *D* and *L*. For biomedical applications, the most commonly used forms are Poly(*L*-lactide) (P*L*LA) and Poly(*D,L*-lactide) P*DL*LA. P*L*LA is a semi-crystalline polymer with high mechanical strength, rendering it a suitable material for load bearing applications. However, its degradation time is slow with total resorption time in excess of 5 years[2–6]. P*DL*LA is more suited to non-load bearing applications, such as drug delivery, due to its amorphous nature and fast degradation time[2–6]. PGA, on the other hand, is highly crystalline with high mechanical strength, however, due to its hydrophilic nature its degradation is rapid, being reported as losing strength after one or two months and complete resorption after 6-12 months[2,3,6].

The ability to tailor polymers to meet required mechanical and/or degradation properties has made them an attractive alternative to their metallic counterparts. The ideal bioresorbable polymer would maintain sufficient mechanical strength during tissue healing (approximately 8-12 weeks depending on the application)[5], then begin to lose mass to allow new tissue to grow, eventually replacing the implanted polymer. One of the most significant challenges in the research of bioresorbable polymers is the development of this type of degradation profile. Copolymerisation of PLA and PGA, forming poly(*L*-lactide-*co*-glycolide) (P*L*LGA) and poly(*D,L*-lactide-*co*-glycolide) (P*DL*LGA), has become increasingly popular for preparation of bone substitute constructs since the use of different copolymer ratios allows greater control of mechanical and physicochemical properties and degradation rates.

Beyond control of copolymer ratio, other approaches to improve the properties of this group of polymers have included self-reinforcement with drawn PLGA fibres[7] to increase modulus and strength, as well as irradiation treatments[8] and chemical crosslinking[9] to alter the degradation behaviour. There is also a plethora of work focusing on fillers used to prepare biocomposites, utilising this group of polymers as the matrix component. Such biocomposites are used commercially in orthopaedic applications, with the most common filler component being hydroxyapatite of beta tricalcium phosphate particles. Despite some commercial marketing claims, there is still limited clinical evidence that biocomposites perform any better than pure copolymers in fracture fixation applications[8,10].

Despite Food and Drug Administration (FDA) approval of devices utilising these copolymers[11] and wide recognition of biocompatibility, there are numerous reports in the literature of a delayed inflammatory reaction occurring months or years after implantation[2,12–16]. This reaction is characterised as a non-specific foreign body reaction and is not specific to polymer type, implant location or subject[2].

The lack of knowledge of the long-term degradation and biocompatibility of these polymers was highlighted by the failures of the CALAXO screw. This was launched in 2006 by Smith and Nephew, for anterior cruciate ligament (ACL) reconstruction, and composed of P*DL*LGA (85:15) with calcium carbonate. This novel screw was designed to overcome the limitations of slow degrading P*L*LA

screws by degrading more rapidly, with the addition of calcium carbonate to neutralise acidic degradation products. However, the positive results of pre-clinical studies[17], with no reported adverse reactions, were not corroborated with clinical trials as a high number of patients presented with adverse reactions occurring between 2-36 weeks of implantation[18]. Due to the unpredictable degradation of the screw and the high number of complications, it was eventually withdrawn from the market in August 2007[10,17–20]. The CALAXO screw example demonstrates the difficulties in developing bioresorbable devices that match the 'ideal' model. Biocomposite polymers composed of P*L*LGA are showing more potential in *in vivo* applications with improved degradation properties and biocompatibility. Smith and Nephew have developed the REGENESORB biocomposite material, composed of P*L*LGA (85:15) combined with calcium sulfate and β-tricalcium phosphate (β-TCP) in a 65:20:15 ratio. This material has been designed to improve upon currently marketed bioresorbable materials and has shown promising results in initial pre-clinical trials[21]. The Milagro screw, developed by Depuy Mitek, composed of 70% PLLGA (85:15) with 30% β-TCP has also demonstrated positive results in clinical trials showing osteoconductivity and good biocompatibility[10,22].

Current *in vitro* tests to assess the degradative changes in physicochemical, mechanical and biological properties of bioresorbable polymers are generally carried out at 37°C in pH 7.4 phosphate-buffered saline (PBS), simulating physiological conditions. It can therefore be difficult to assess the long-term degradation properties of polymers that take months, or years to degrade at physiological temperature. Temperature accelerated degradation has shown potential as a method that can be used to extrapolate accelerated test results back to physiological conditions[4,23–26]. This study aims to develop an increased temperature accelerated degradation methodology that can be used to simulate the long-term degradation of P*DL*LGA (85:15) and P*L*LGA (85:15) over a practical time period. The novelty of this work lies in the fact that the optimal accelerated degradation conditions and associated reaction constants where previously unavailable. Furthermore, where elevated temperature conditions have been previously utilised there has not been a detailed comparison to physiological temperature, which is clearly essential for validation purposes, nor between crystalline and amorphous polymers of otherwise similar nature. Such pre-conditioning of these polymers would be valuable as a method to prepare samples for an *in vitro* experimental evaluation to assess cell response to degradative changes, for example providing insight into the potential to a cause delayed inflammatory response at different stages of degradation. The methodology developed is therefore proposed as a means to provide a better understanding of the causes of the adverse reactions that occur with the use of bioresorbable polymers.

2 Materials and Methods

2.1 Materials

P*DL*LGA 85:15 (PURASORB PDLG 8531, Corbion Biomaterals, the Netherlands) and P*L*LGA 85:15 (PURASORB PLG 8531, Corbion Biomaterials, the Netherlands) in pellet form were used for this study. The residual monomer content of P*DL*LGA and P*L*LGA, is approximately 2% and 0.1% respectively, in accordance with their certificate of analysis. Materials were stored in a freezer (-20°C) in sealed packaging until use.

2.2 Sample Preparation

P*DL*LGA and P*L*LGA pellets were compression moulded using a Collins P200P Platen Press. A mass of 14.5g of either P*DL*LGA or P*L*LGA was placed in a 100x100x1mm^3 mould. Two sheets of commercially available silicone baking parchment (Lakeland) were placed on either side of the mould to prevent the polymer sticking to the metal compression plates during compression moulding. Samples were compression moulded using the heating cycle in Table 1.

Table 1. Platen press heating cycle for compression moulding of PDLLGA and PLLGA

Phase	**1**	**2**	**3**
Temperature (°C)	180	180	180
Pressure (bar)	0	2	10
Time (s)	180	60	150

P*L*LGA compression moulded sheets were then annealed in an oven for 4h at 100°C (P*DL*LGA was not annealed, as this was considered unnecessary due to its amorphous nature). P*DL*LGA and P*L*LGA disc-shaped samples with 1 mm thickness and 8mm diameter were produced from the sheets using an FB 1800 50W laser cutting machine. Samples were stored in a desiccator until required.

2.3 *In Vitro* Degradation

The initial mass, m_0, of the samples was recorded. Under sterile conditions in a Class II biosafety hood, samples were washed in ethanol then rinsed with sterile PBS, before being fully immersed in 10mL sterile PBS in sealed containers (one sample per container) with a volume to mass ratio of approximately 140:1, in accordance with ISO 13781:2017. Both the P*DL*LGA and P*L*LGA sample containers were divided into 4 groups and placed in separate air-circulating ovens set at 37°C, 47°C, 57°C and 70°C for the durations shown in Table 2. These choices of temperature were based on 37°C to reflect physiological temperature and then 47°C and 57°C to utilise steps of 10°C above physiological temperature, following the recommendations of Hukins et al[27]. Furthermore, 70°C was selected for the study to allow comparisons to be made to previous work by Weir et al[4]. PBS solutions were not changed during the degradation timeframe.

Table 2. Accelerated degradation time points for PDLLGA and PLLGA at 37°C, 47°C, 57°C and 70°C

P*DL*LGA				**P*L*LGA**			
37°C (days)	*47°C (days)*	*57°C (days)*	*70°C (days)*	*37°C (days)*	*47°C (days)*	*57°C (days)*	*70°C (days)*
7	3	1	0.2	28	7	7	7
14	5	2	0.7	42	14	14	14
21	7	3	1	56	28	28	21
28	10	4	1.2	70	42	45	28
35	12	7	2	91	57	50	70
41	14		3	169	64	57	
48	21			256	70	64	
55				357	78	78	
63					98	91	
69					112		
76							
84							
91							

2.4 Characterisation

2.4.1 Mass change

At each time point the pH of the solution was recorded. On retrieval, the samples were rinsed with distilled water, dried with Kimtech science precision dry wipes to remove surface moisture and weighed to determine the wet mass (m_w). The samples were subsequently dried in a vacuum oven for 72h at 30°C and 600 mmHg and reweighed to determine the dry mass (m_d). The percentage mass loss at each time point was calculated after drying using equation (1) and the percentage swelling was calculated using equation (2).

$$\%\ Mass\ Loss = \frac{m_0 - m_d}{m_0} x100\% \quad (1)$$

$$\%\ Swelling = \frac{m_w - m_d}{m_d} x100\% \quad (2)$$

2.4.2 Gel permeation chromatography (GPC)

GPC was used to determine changes in molecular weight during the polymer degradation. Experiments were performed using an Agilent Technologies 1260 Infinity SEC system comprising a guard column and two Agilent PL gel 5μm MIXED-C columns operating at 25 °C. The eluting solvent was tetrahydrofuran (THF) containing 2.0% v/v triethylamine and 0.05% w/v butylated hydroxytoluene (BHT) inhibitor, with a flow rate of 1 mL/min. A refractive index detector operating at 30°C was used. The instrument was calibrated using ten Agilent EasiVial poly(methyl methacrylate) standards with molecular weights of 1010, 1950, 6850, 13 900, 31 110, 68 750, 137 800, 320 000, 569 000 and 1 048 000 g/mol. Samples were prepared with a polymer concentration of 3 mg/mL and left overnight on a magnetic stirrer. The resulting solutions were then filtered using a syringe filter (0.45μm) and were placed into vials with 1 drop of dimethyl sulfoxide (DMSO) added as the GPC flow rate marker. The samples were analysed using Cirrus GPC software and their number average molecular weight (*Mn*), weight average molecular weight (*Mw*) and polydispersity index (PDI) value were determined.

2.4.3 Differential Scanning Calorimetry (DSC)

DSC (Q200, TA Instruments, Leatherhead, UK) was used to analyse changes in thermal behaviour during degradation. The DSC was calibrated using an indium standard and nitrogen purge gas with a flow rate of 60 mL/min. Samples (8-10mg) were analysed in standard aluminium pans over a temperature range of -20°C to 200°C and a heating rate of 10°C/min in a two stage heating phase. Data was analysed using Universal Analysis software (TA instruments) providing measurements of glass transition temperature (*Tg*), melting temperature (*Tm*) and enthalpy of fusion (ΔH_{melt} J/g). The *Tg* was defined as the midpoint of the transition, and the *Tm* was determined and reported as the peak temperature. In cases where a double peak is observed the highest peak is reported as the *Tm*. Equation (3) was used to calculate the % crystallinity of P*L*LGA, using the ΔH_{melt} values obtained for P*L*LGA relative to the ΔH_{melt} of a 100% crystalline sample of P*L*LA, ΔH_{melt} = 93 J/g[28], as a ΔH_{melt} for a 100% crystalline sample P*L*LGA is not available.

$$\%\ Crystallinity = \frac{\Delta H_{melt}\ (J/g)}{93\ (J/g)} \times 100\% \quad (3)$$

3 Modelling Degradation

3.1 Uncatalysed Model

A statistical model developed by Anderson[29] relates the change in molecular weight, until the point of mass loss, to the rate of hydrolysis according to equation (4):

$$^{1}/_{Mn_t} = {}^{1}/_{Mn_o} + kt \quad (4)$$

Where Mn_t = *Mn* at time *t*; Mn_0 = *Mn* at *t* = 0; *k* = rate constant; and *t* = time.

This equation is derived on the basis that *Mn* is directly proportional to polymer chain scission.

3.2 Auto-catalysed Model

It is well understood that the hydrolysis of polyesters is accelerated by autocatalysis with the rate of reaction dependent on the concentration of the carboxylic acid end groups [COOH][24,30–32]. Pitt et al[33] proposed the kinetics of the auto-catalysed hydrolytic reaction according to equation (5):

$$d[E]/_{dt} = {}^{-d[COOH]}/_{dt} = -k'[COOH][H_2O][E] \quad (5)$$

Where [COOH], [H_2O] and [E] are the carboxyl end group, water and ester concentrations in the polymer matrix, respectively. By assuming the water and ester concentration remain constant and [COOH] = 1/*Mn* the following relationship can be derived:

$$-d[COOH]/_{dt} = -k'[COOH][H_2O][E]$$

$$-\int_{\frac{1}{Mn_0}}^{\frac{1}{Mn_t}} \frac{1}{[COOH]}\, d[COOH] = -k' \int_0^t dt$$

$$-\left(\ln\frac{1}{Mn_t}-\ln\frac{1}{Mn_0}\right)=-k't$$

$$\ln\frac{Mn_t}{Mn_0}=-k't \quad (6)$$

$$Mn_t=Mn_0e^{-k't} \quad (7)$$

3.3 Arrhenius Equation

The Arrhenius equation was used to determine whether degrading P*DL*LGA or P*L*LGA at elevated temperatures could be used to predict the degradation at physiological temperature:

$$k''=Ae^{-E_a/RT} \quad (8)$$

Where *k''* = rate constant, *A* = constant, E_a = activation energy (J/mol), *R* = universal gas constant (8.314J/molK), *T* = temperature (K).

$$\ln k''=-\left(\frac{E_a}{R}\right)\left(\frac{1}{T}\right)+\ln A \quad (9)$$

If the reaction obeys the Arrhenius equation (9) a linear relationship should be observed.

4 Results

4.1 Visual Inspection

P*DL*LGA and P*LL*GA samples have a translucent off-white colour and during degradation they turn opaque and white. P*DL*LGA (Figure 1a) underwent significant changes to its appearance throughout degradation. After 28 days at 37°C, 5 days at 47°C, 1 day at 57°C and 0.2 days at 70°C, the samples became visibly damaged. After 57 days at 37°C, 10 days at 47°C and 2 days at 57°C, the samples appeared visibly swollen with a hard exterior and viscous liquid interior. After 78 days at 37°C, 12 days at 47°C, 3 days at 57°C and 0.7 days at 70°C, the samples turned into a viscous liquid. These degradation characteristics are consistent with the mechanism of heterogenous degradation, first proposed by Grizzi et al[34]. In contrast, P*L*LGA (Figure 1b) samples remained translucent until 57 days at 47°C, 7 days at 57°C and 7 days at 70°C where they turned opaque and white. The samples appeared volumetrically unchanged even after 112 days at 47°C, 91 days at 57°C and 28 days at 70°C but became fragile and disintegrated into a powder on handling when opaque and white in appearance. P*L*LGA samples degraded at 37°C showed little change in appearance after 357 days.

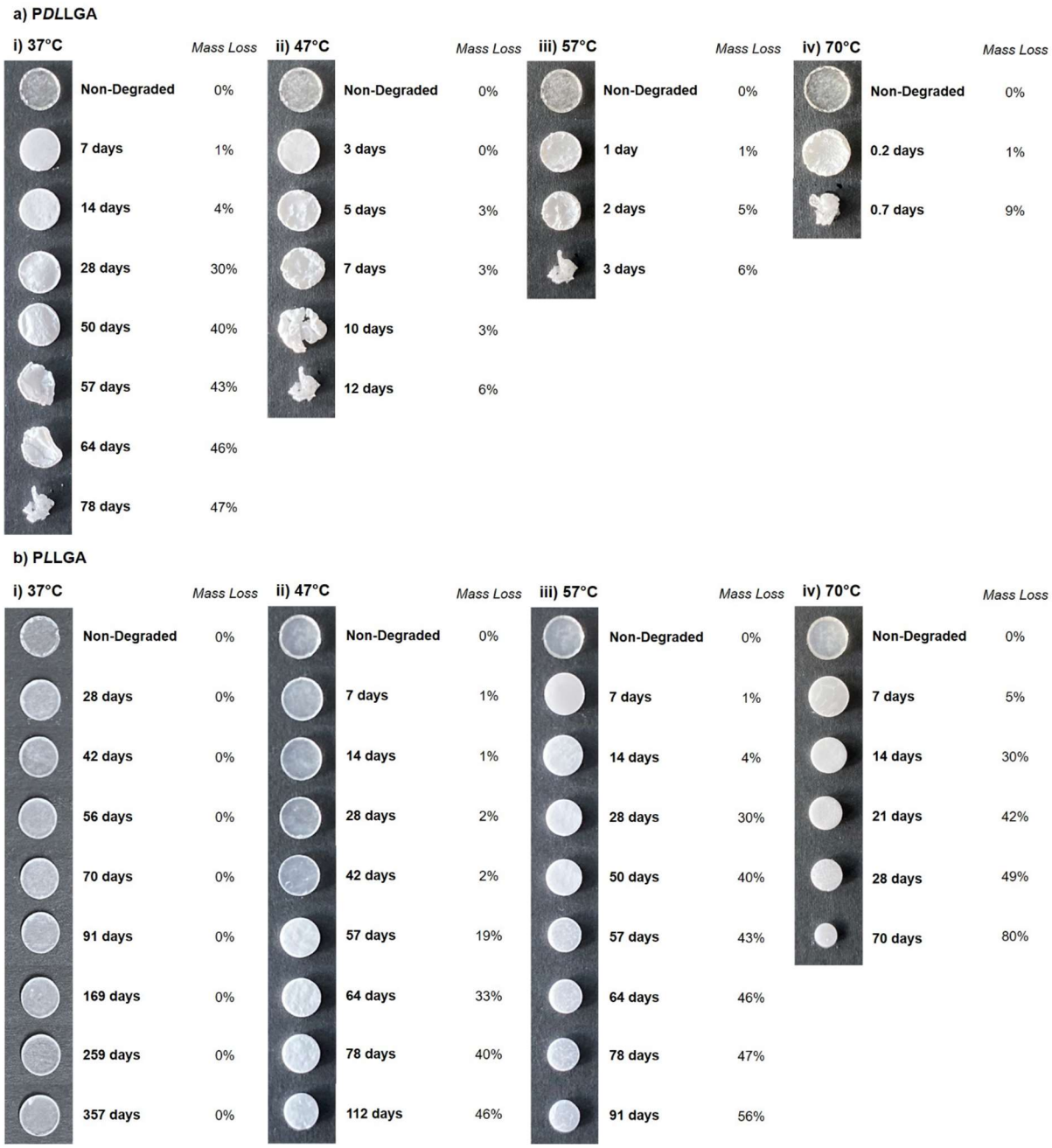

Figure 1. Sample appearance of a) PDLLGA and b) PLLGA after degradation at i) 37°C, ii) 47°C, iii) 57°C and iv) 70°C

4.2 Change in pH with Degradation

The pH of PBS buffer was monitored throughout degradation. For P*DL*LGA (Figure 2a), there was a slow decrease in pH from 7.4 to approximately 6.3 after 55 days at 37°C, 12 days at 47°C, 4 days at 57°C and 1 day at 70°C. This was then followed by a rapid decline to approximately pH 2.8 after 69 days at 37°C, 21 days at 47°C, 7 days at 57°C and 3 days at 70°C. For P*L*LGA (Figure 2b), initially a slow decrease in pH was observed with a decrease to pH 6.4 after 357 days at 37°C, pH 6.0 after 42 days at 47°C, pH 5.9 after 14 days at 57°C and pH 5.4 after 7 days at 70°C. Similar to P*DL*LGA, this was then followed by a more rapid decline to pH 2.8 after 57 days at 47°C, 28 days at 57°C and 14 days at 70°C. However, no decrease in pH was observed for samples degraded at 37°C, which was

considered to be due to the fact that the polymer had not sufficiently degraded over the timeframe of the experiment to start significantly releasing oligomers (of acidic nature) into the PBS medium.

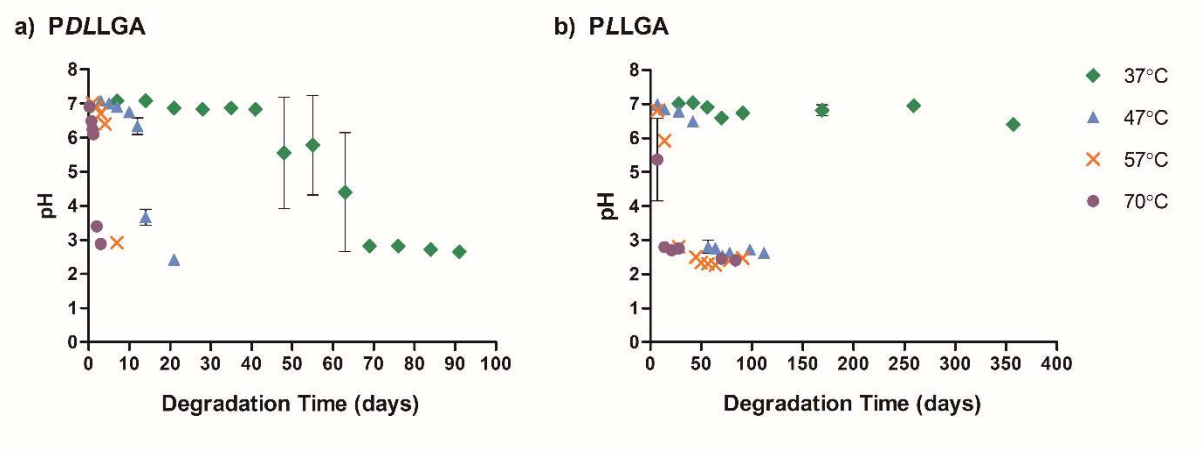

Figure 2. pH versus degradation time of a) PDLLGA and b) PLLGA at 37°C, 47°C, 57°C and 70°C (Ave ± std. dev.)

4.3 Mass Change versus Degradation Time

The mass of P*DL*LGA and P*L*LGA after drying was decreased during degradation at 37°C, 47°C, 57°C and 70°C. For P*DL*LGA (Figure 3a), a maximum mass loss of 70% after 91 days at 37°C, 94% after 21 days at 47°C, 36% after 7 days at 57°C and 72% after 3 days at 70°C was recorded. For P*L*LGA (Figure 3b), a maximum mass loss of 5% after 357 days at 37°C, 46% after 112 days at 47°C, 56% after 91 days at 57°C and 80% after 70 days at 70°C was recorded.

Swelling of P*DL*LGA (Figure 4) occurred immediately upon immersion in PBS buffer, with the rate of swelling faster at higher temperatures. A maximum swelling of 141% after 91 days at 37°C, 97% after 10 days at 47°C, 43% after 3 days at 57°C and 117% after 1.2 days at 70°C was observed. However, swelling occurred without significant mass loss, for example when the percentage swelling was 96% at 37°C, 97% at 47°C, 43% at 57°C and 97% at 70°C mass loss was 6%, 3%, 6% and 9%, respectively. Figure 5 shows that swelling of P*L*LGA does not occur immediately upon immersion in PBS buffer but gradually increases during degradation. A maximum swelling of 3% after 357 days at 37°C, 61% after 112 days at 47°C, 91% after 91 days at 57°C and 51% after 21 days at 70°C was observed. Unlike P*DL*LGA, mass loss in P*L*LGA almost replicated the amount of polymer swelling (figure 5).

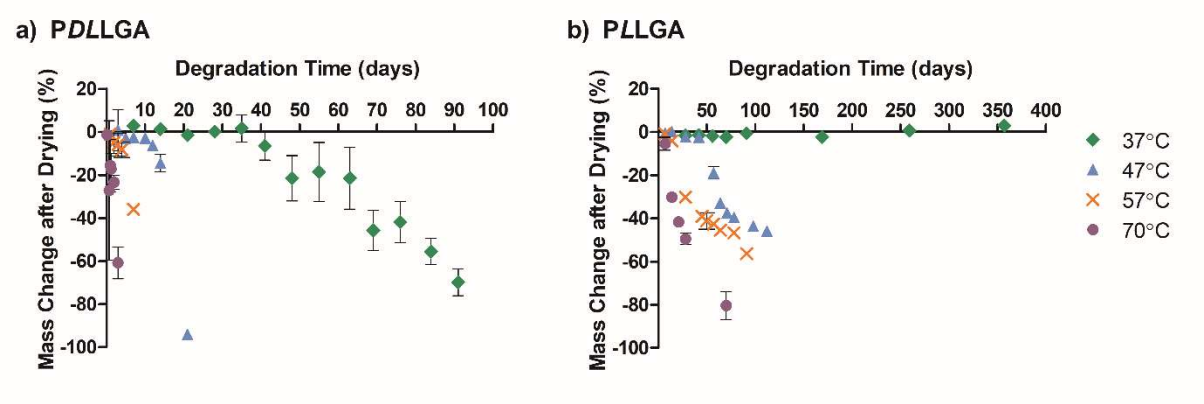

Figure 3. Percentage mass change after drying versus degradation time of a) PDLLGA and b) PLLGA at 37°C, 47°C, 57°C and 70°C (Ave ± std. dev.)

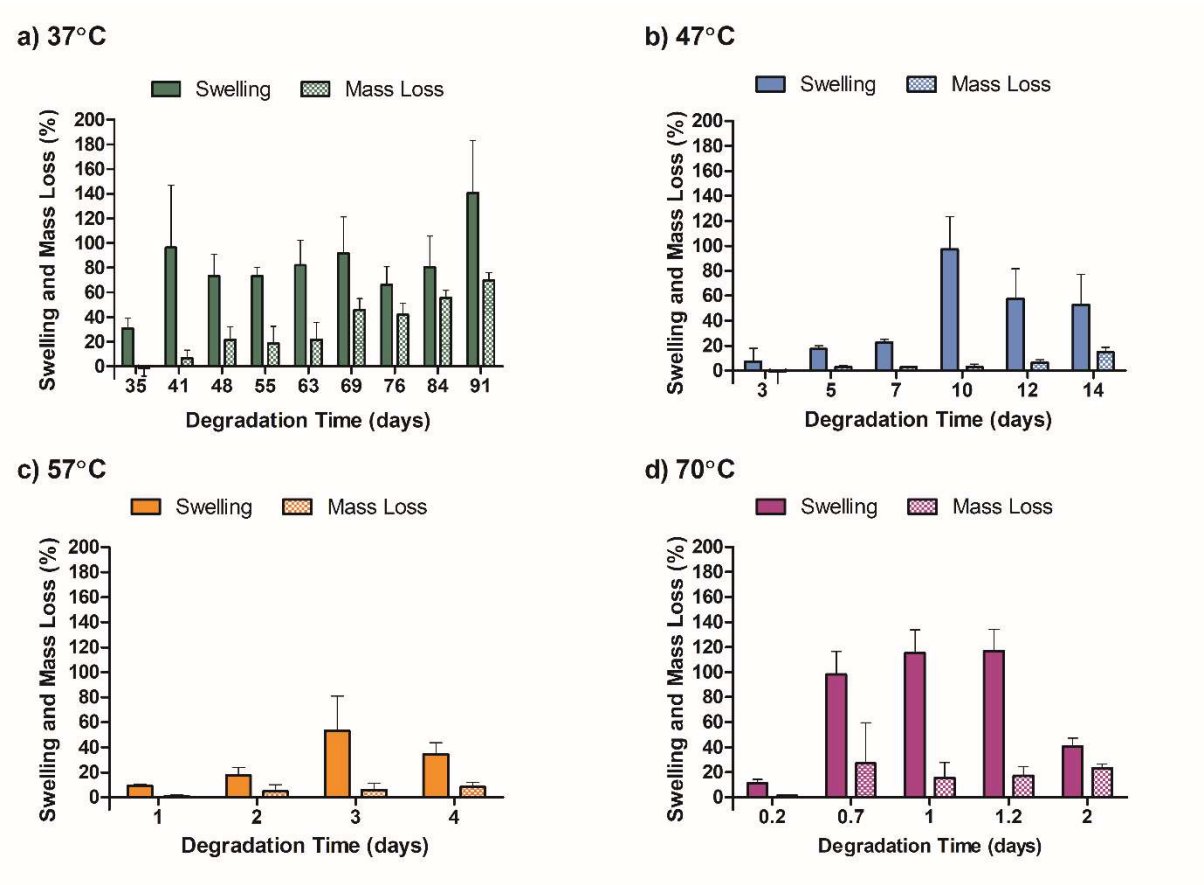

Figure 4. Percentage swelling versus mass loss of PDLLGA at a) 37°C, b) 47°C, c) 57°C, d) 70°C (Ave ± std. dev.)

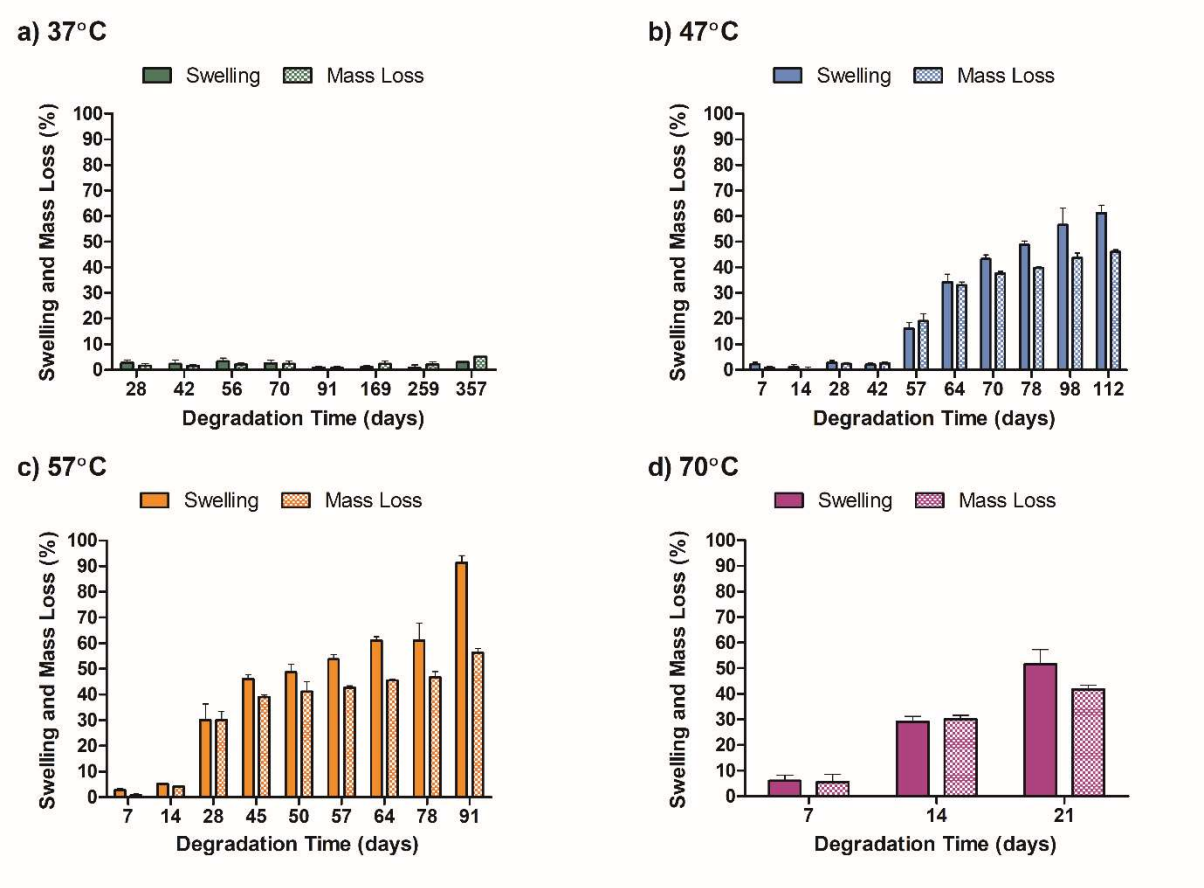

Figure 5. Percentage swelling versus mass loss of PLLGA at a) 37°C, b) 47°C, c) 57°C, d) 70°C (Ave ± std. dev.)

4.4 Thermal Properties

The DSC thermographs of the second heating cycle of P*DL*LGA and P*L*LGA are presented in Figures 6 and 7, respectively. Significant declines in the T*g* of P*DL*LGA were observed during degradation at all temperatures used, 37°C, 47°C, 57°C and 70°C (Table 3). The reduction seems to start immediately upon immersion in PBS buffer. There is a general trend of decreasing T*g* and T*m* with increasing crystallinity during the degradation of P*L*LGA *at* 37°C, 47°C, 57°C and 70°C (Table 4). A significant drop in the T*g*, from 58.3°C, occurs after 42 days at 47°C (T*g* = 37.7°C), 14 days at 57°C (T*g* = 44.9°C) and 7 days at 70°C (T*g* = 46.5°C), which coincides with an increase in crystallinity from zero to 12%, 18% and 17%, respectively. At 37°C, the T*g* of P*L*LGA declined by 1.3°C after 357 days, with no crystallisation occurring.

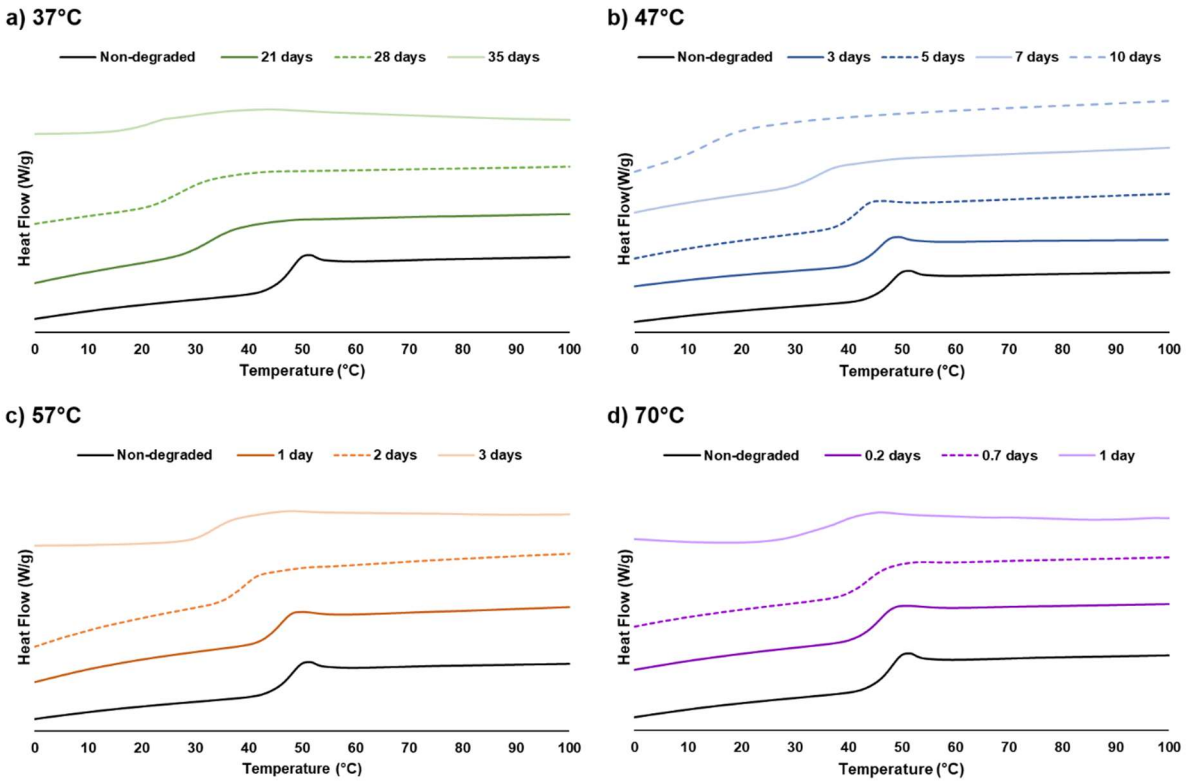

Figure 6. DSC thermograms showing second heating cycle of PDLLGA during degradation at 37°C, 47°C, 57°C and 70°C.

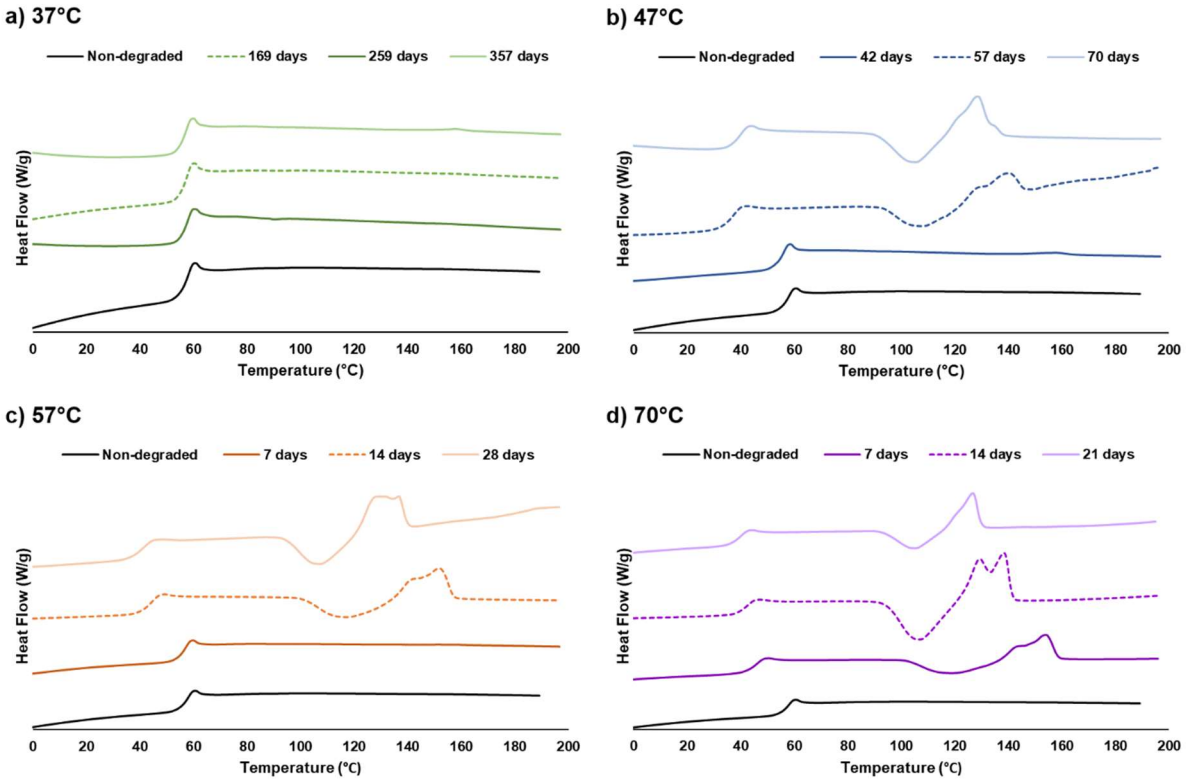

Figure 7. DSC thermograms showing second heating cycle of PLLGA during degradation at 37°C, 47°C, 57°C and 70°C

Table 3. Thermal properties of PDLLGA during degradation at 37°C, 47°C, 57°C and 70°C

37°C	*Degradation Time (days)*	0	21	28	35
	Tg (°C)	48.3	33.8	31.8	16.4
47°C	*Degradation Time (days)*	0	3	5	7
	Tg (°C)	48.3	46.0	41.7	34.0
57°C	*Degradation Time (days)*	0	1	2	3
	Tg (°C)	48.3	45.7	39.0	31.1
70°C	*Degradation Time (days)*	0	0.2	0.7	1
	Tg (°C)	48.3	46.7	43.4	41.7

Table 4. Thermal properties of PLLGA during degradation at 37°C, 47°C, 57°C and 70°C

37°C	*Degradation Time (days)*	0	169	256	357
	Tg (°C)	58.3	58.0	58.0	57.0
	Tm (°C)	-	-	-	-
	Crystallinity (%)	-	-	-	-
47°C	*Degradation Time (days)*	0	42	57	70
	Tg (°C)	58.3	56.0	37.3	40.1
	Tm (°C)	-	158.0	138.9	128.7
	Crystallinity (%)	-	1	12	15
57°C	*Degradation Time (days)*	0	7	14	28
	Tg (°C)	58.3	57.1	44.9	42.1
	Tm (°C)	-	-	151.9	128.2
	Crystallinity (%)	-	-	18	22
70°C	*Degradation Time (days)*	0	7	14	21
	Tg (°C)	58.3	46.5	43.0	40.5
	Tm (°C)	-	154.0	138.4	126.8
	Crystallinity (%)	-	17	33	15

4.5 Molecular Weight Distribution

The *Mn* and the PDI values of P*DL*LGA and P*L*LGA observed during their degradation are presented in Tables 5 and 6. The initial molecular weight of P*L*LGA was higher (*Mn* = 135 000) than that of P*DL*LGA (M*n* = 27 800) and it is evident that the degradation of P*L*LGA is slower. As expected, the molecular weight of both polymers decreased with degradation time. The P*DL*LGA molecular weight distributions (MWDs) obtained by GPC (Figure 8), demonstrate how the polymer molecular weight changed during degradation at 37°C, 47°C, 57°C and 70°C. The GPC chromatogram of the non-degraded P*DL*LGA appears to have a small peak at high elution time (at 19.3-20.5 min) in addition to

the polymer peak at approximately 11.5-17 min, attributed to residual monomer. Residual monomer is unreacted monomer that remain within the polymer matrix after polymerisation or other processing techniques[35]. The initial (virgin) non-degraded polymer contains a maximum of 2% residual monomer, according to its certificate of analysis. At each temperature there is a shift of the main polymer peak towards higher elution times, which correspond to lower molecular weights, as degradation time increases. During degradation, P*DL*LGA is broken down into oligomers and monomers, shown in red boxes A, B, C and D on each graph in Figure 8. Their amount is increased during degradation as evident by the observed increase in the refractive index signal and the area under the monomer peaks A-D with degradation time. This is most notable at 37°C and 47°C, as after 35 days and 12 days, respectively, the P*DL*LGA samples appear to have high amounts of short chain polymer (oligomers) and monomers.

The MWDs of P*L*LGA observed at different times also show polymer degradation over time, with a shift of the peak maximum to higher elution times in the GPC chromatograms (Figure 9). At 37°C and 47°C the decline in molecular weight is initially slow. At 47°C (Figure 9b), there is a large shift of the peak maximum to higher elution times between 42 and 57 days, where the higher molecular weight chains at 42 days (*Mn* = 22 700, *Mw* = 80 000) have almost completely disappeared into the shorter molecular weight chains at 57 days (*Mn* = 2000, *Mw* = 5060). The peak molecular weight (*Mp*) decreased by 78% after 42 days (*Mp* = 78 500) and 99% after 57 days (*Mp* = 3440) from its initial value (*Mp* = 351 000). At 57°C and 70°C, the decline of molecular weight is faster, with *Mp* decreasing by 96% after 14 days (*Mp* = 12 600) and 7 days (*Mp* = 14 900), respectively. At the later stages of the P*L*LGA degradation, shoulders to lower elution times appeared on the chromatogram peaks after 57 days at 47°C, 28 days at 57°C and 14 days at 70°C. The peaks become less uniform as the length of chains within the polymer become more varied due to random chain scission of the polymer. This is only observed in the semi-crystalline P*L*LGA and can be attributed to differences in the degradation rates of the amorphous and crystalline regions of the polymer[36,37]. The residual monomer content, presented in the certificate of analysis, in the initial P*L*LGA is approximately 0.1%, which is significantly lower than that of P*DL*LGA. It is clear from the MWD of the non-degraded P*L*LGA that the polymer has a small amount of residual monomer evident from the small peak at elution times of 19-20.5min and as it degrades there is a slight increase in the amount of residual monomer (shown in red boxes E, F, G and H on each graph).

Table 5. Molecular weights and PDI values of PDLLGA during degradation at 37°C, 47°C, 57°C and 70°C

37°C	*Degradation Time (days)*	0	7	14	21	28	35
	Mn (g/mol)	27 800	9810	6780	2620	2170	1480
	PDI value	3.37	4.37	3.88	3.77	3.97	4.37
47°C	*Degradation Time (days)*	0	3	5	7	10	12
	Mn (g/mol)	27 800	9400	3390	1980	1160	645
	PDI value	3.37	3.18	4.15	3.41	2.32	1.37
57°C	*Degradation Time (days)*	0	1	2	3		
	Mn (g/mol)	27 800	8750	3600	2000		
	PDI value	3.37	3.95	3.35	2.93		
70°C	*Degradation Time (days)*	0	0.2	0.7	1		
	Mn (g/mol)	27 800	15 200	3510	2060		
	PDI value	3.37	2.57	3.15	2.93		

Table 6. Molecular weights and PDI values of PLLGA during degradation at 37°C, 47°C, 57°C and 70°C

37°C	*Degradation Time (days)*	0	28	42	56	70	91	169	259	357
	Mn (g/mol)	135 000	124 000	128 000	121 000	125 000	104 000	102 000	85 900	64 700
	PDI value	2.88	3.06	2.83	2.98	2.81	3.38	2.88	2.73	2.33
47°C	*Degradation Time (days)*	0	7	14	28	42	57	64	71	78
	Mn (g/mol)	135 000	113 000	108 000	60 200	22 700	2000	1570	1400	1280
	PDI value	2.88	3.07	2.68	2.96	3.53	2.54	2.18	2.00	1.93
57°C	*Degradation Time (days)*	0	7	14	28	45	50	57	64	
	Mn (g/mol)	135 000	43 000	3920	1680	792	767	740	703	
	PDI value	2.88	3.26	3.55	1.91	2.30	2.28	2.20	2.17	
70°C	*Degradation Time (days)*	0	7	14	21	28				
	Mn (g/mol)	135 000	4410	1880	1390	1260				
	PDI value	2.88	3.37	2.19	1.54	1.50				

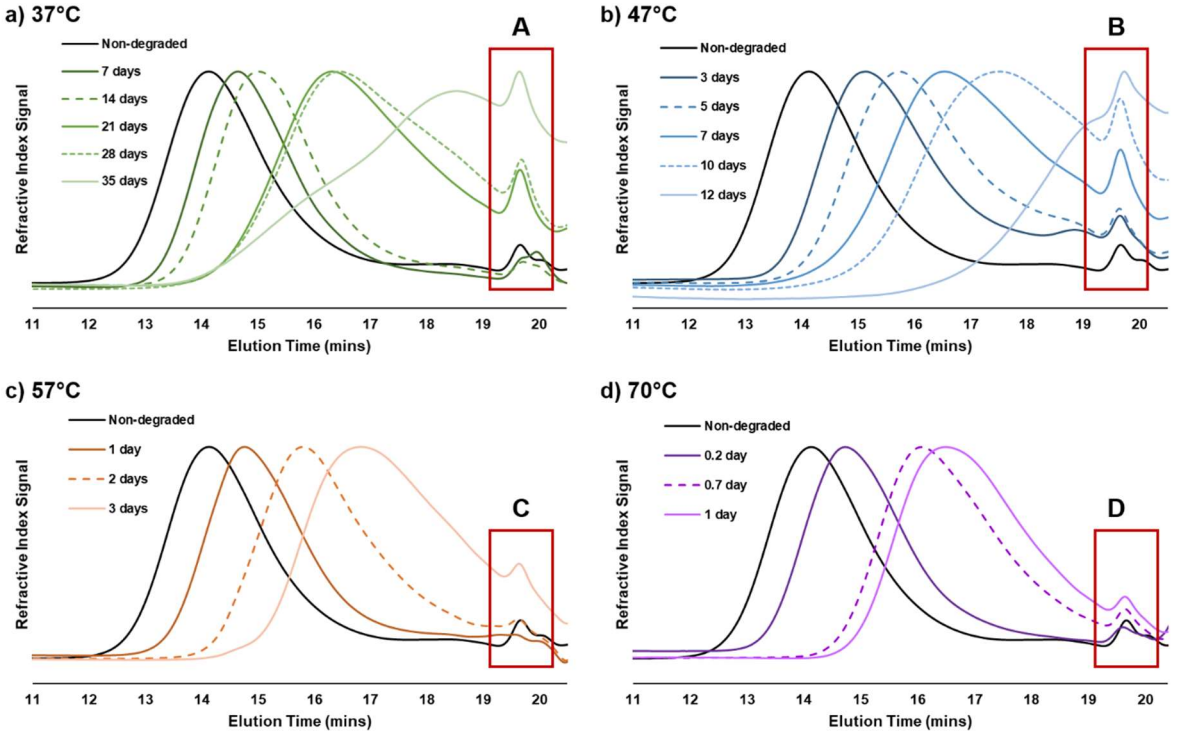

Figure 8. GPC (THF) chromatograms of PDLLGA during degradation at a) 37°C, b) 47°C, c) 57°C and d) 70°C. Monomer peaks shown in red boxes labelled A, B, C and D.

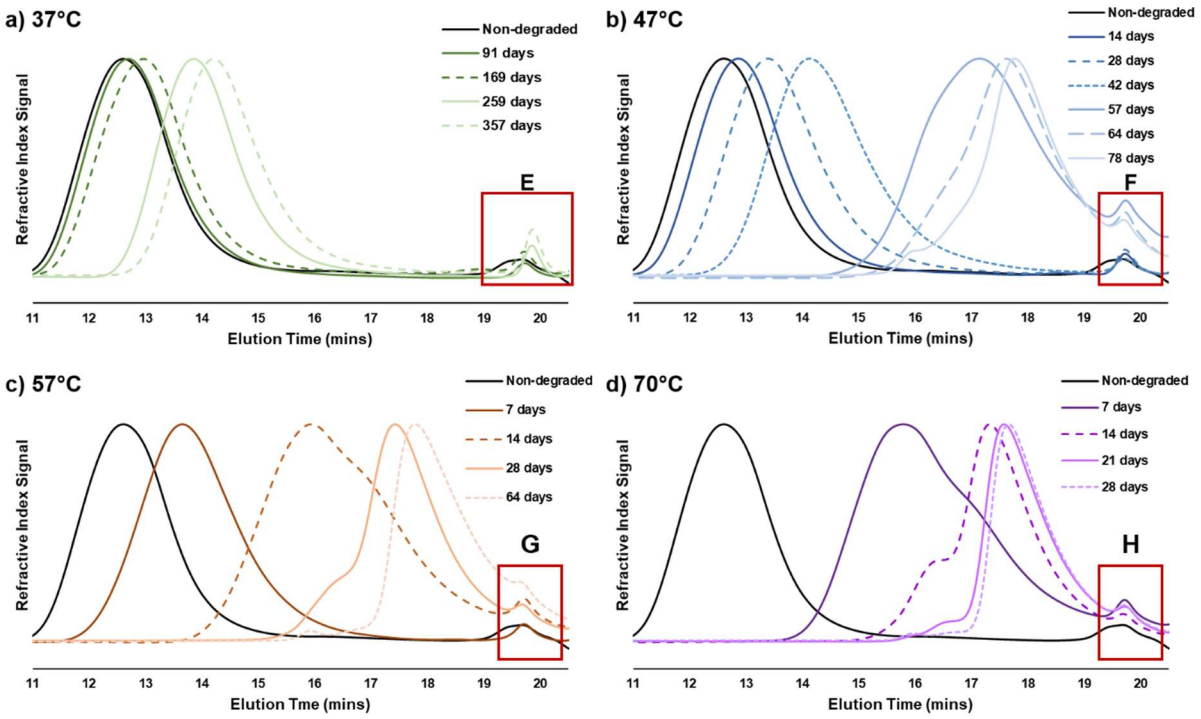

Figure 9. GPC (THF) chromatograms of PLLGA during degradation at a) 37°C, b) 47°C, c) 57°C and d) 70°C. Monomer peaks shown in red boxes labelled E, F, G and H.

5 Discussion

5.1 Selection of Increased Temperature to Accelerate Degradation

To determine whether degradation accelerated by increased temperature is predictive of 'real-time' analysis at 37°C, a range of temperatures (47°C, 57°C and 70°C) above and below the polymers' *Tg* (50-55°C[6,38]) were selected. Figure 10 shows the change in *Mn* of P*DL*LGA and P*L*LGA with degradation time, where the data for the range of temperatures tested have been superimposed. It is evident from Figure 10a that the *Mn* of P*DL*LGA at 37°C, 47°C, 57°C and 70°C decreases with degradation time. As expected, the rate of degradation is faster at higher temperatures, with a 92% decrease in *Mn* after 28 days at 37°C, in comparison to a 93% decrease after 7 days at 47°C, 3 days at 57°C and 1 day at 70°C. The degradation profile of P*DL*LGA shows that initially there is a rapid decrease in molecular weight followed by a period of slow molecular weight loss. The degradation time of P*L*LGA is significantly slower than P*DL*LGA, this may be due to the higher initial molecular weight, its more crystalline structure or its lower residual monomer content[35,36,39,40]. Figure 10b also shows that the *Mn* of P*L*LGA decreases with degradation time. At 57°C and 70°C the *Mn* decreased by 97% after 14 days and 7 days, respectively. At 47°C the *Mn* decreased by 83% after 42 days and at 37°C the *Mn* decreased by 52% after 357 days. The rate of degradation is faster at higher temperatures. At 47°C, 57°C and 70°C there is a rapid decrease of molecular weight followed by a period of slow decline, this is consistent with poly(α-hydroxy acids)[23,36,41]. However, at 37°C the initial decrease of molecular weight is slow. Analysis of the relationship between the change in mass after drying and *Mn* (Figure 11) shows a clear trend that mass loss is only observed when the *Mn* drops below approximately 1150–3600 g/mol in P*DL*LGA and 1200–4400 g/mol in P*L*LGA. A similar relationship is also observed when considering the decline of T*g* with *Mn* (Figure 12).

The rate of change of *Mn* of P*DL*LGA and P*L*LGA at each temperature was modelled using equations (4) and (6) for the un-catalysed and auto-catalysed degradation models, respectively. The rate constants k_1 and k_2, for P*DL*LGA and P*L*LGA, respectively, were calculated from the linear regression plot of ($1/Mn_t - 1/Mn_0$) versus degradation time for the un-catalysed model (Figure 13). The rate constants k_3 and k_4, for P*DL*LGA and P*L*LGA, respectively, were calculated from the linear regression plot of $\ln(Mn_t/Mn_0)$ versus degradation time for the auto-catalysed model (Figure 14). All rate constants are presented in Table 7. As expected, the rate of hydrolysis is faster at higher temperatures. The rates of hydrolysis of P*DL*LGA at 47°C, 57°C and 70°C, compared to 37°C, for the un-catalysed and auto-catalysed degradation models were similar. Considering the rate constants k_1 and k_3, the rate of hydrolysis of P*DL*LGA at 47°C, 57°C and 70°C increased by approximately x4, x10 and x20, respectively, using the un-catalysed degradation model and x4, x10.7 and x34.9, respectively, using the auto-catalysed degradation model. There were high correlation coefficients (R^2 value) at each temperature, which generally increased as temperature increased. However, the rates of hydrolysis of P*L*LGA at 47°C, 57°C and 70°C, compared to 37°C, for the un-catalysed and auto-catalysed degradation models were significantly different. Considering the rate constants k_2 and k_4, the rate of hydrolysis of P*L*LGA at 47°C, 57°C and 70°C increased by x40, x1000 and x2000, respectively, using the un-catalysed degradation model and x21.9, x133.1 and x160.8, respectively, using the auto-catalysed degradation model. The higher rate of hydrolysis of P*DL*LGA compared to P*L*LGA is most likely due to the differences in the crystallinity of the polymers. The rate constants (k_1, k_2, k_3 and k_4) were plotted according to equation 9 in the form of ln(k) versus 1/T for the un-catalysed and auto-catalysed models (Figure 15). There is a clear linear relationship for the un-catalysed and auto-catalysed models for P*DL*LGA with very high R^2 values of 0.9659 and 0.9947, respectively. The activation energy calculated for the un-catalysed and auto-catalysed models of P*DL*LGA was 79.9kJ/mol and 94.3kJ/mol, respectively. The R^2 values for P*L*LGA were 0.9126 and 0.8509 for the un-catalysed and auto-catalysed models, respectively. The R^2 values for P*L*LGA represent a strong correlation, however, it is not as good a fit compared to P*DL*LGA, suggesting there is some error in the data. The higher degree of experimental error may have occurred due to the long degradation time of P*L*LGA at 37°C. The models were calculated using the *Mn* until the point of mass loss, however, a large decrease in *Mn* did not occur after the latest time point, 357 days at 37°C. It is possible the error has occurred in the final *Mn* value used in the un-catalysed and auto-catalysed models at 37°C, as it is likely this value should be lower. The activation energies calculated for the un-catalysed and auto-catalysed models of P*L*LGA were 208.7 kJ/mol and 136.4 kJ/mol, respectively.

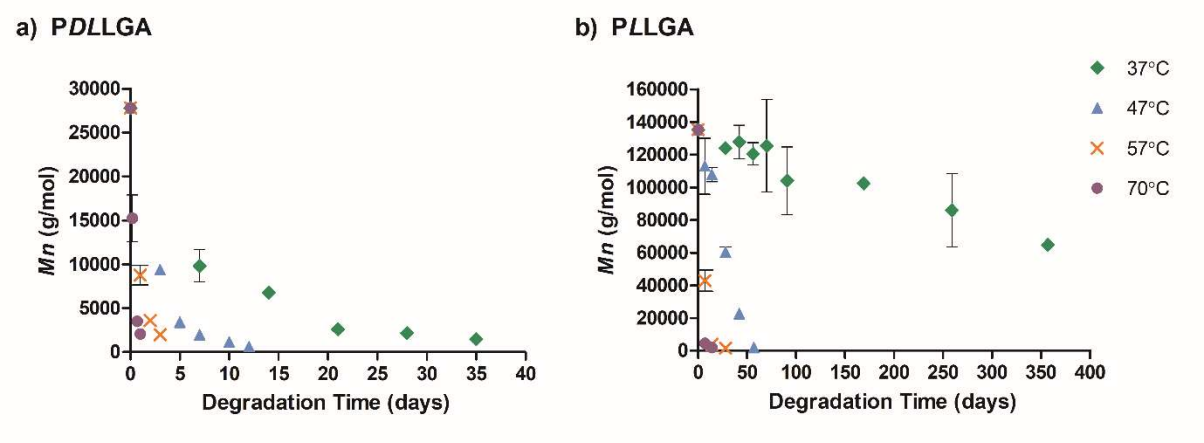

Figure 10. Mn values by GPC (THF) versus degradation time for a) PDLLGA and b) PLLGA at 37°C, 47°C, 57°C and 70°C (Ave ± std. dev.)

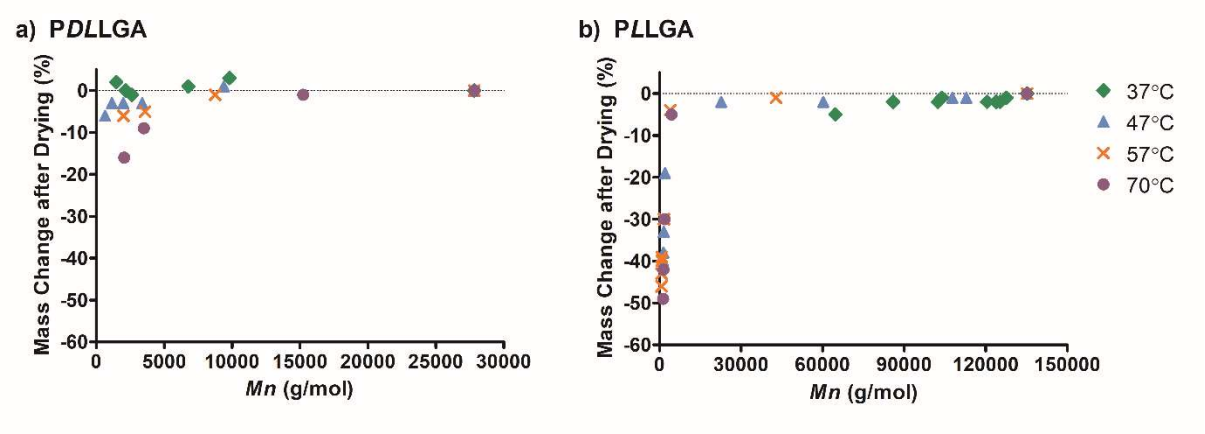

Figure 11. Relationship between percentage mass change after drying and Mn of a) PDLLGA and b) PLLGA at 37°C, 47°C, 57°C and 70°C

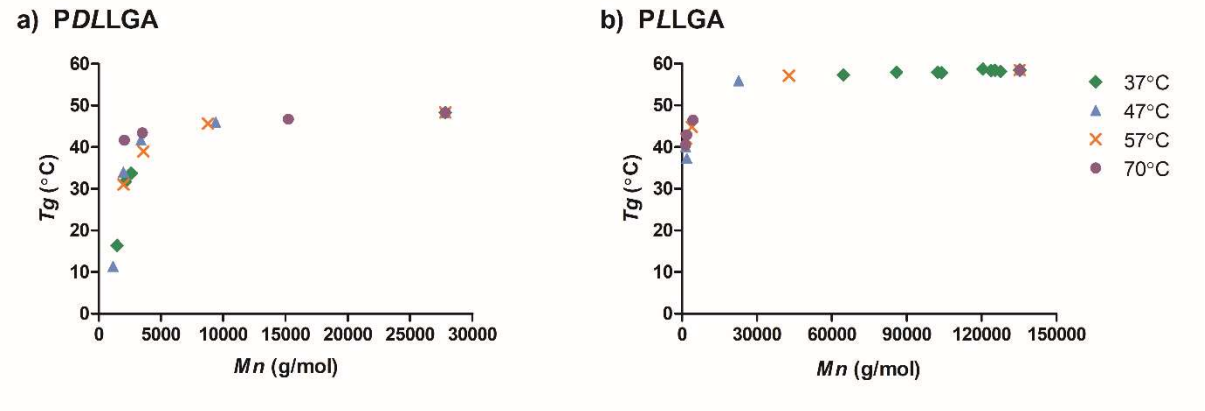

Figure 12. Relationship between Tg and Mn of a) PDLLGA and b) PLLGA at 37°C, 47°C, 57°C and 70°C

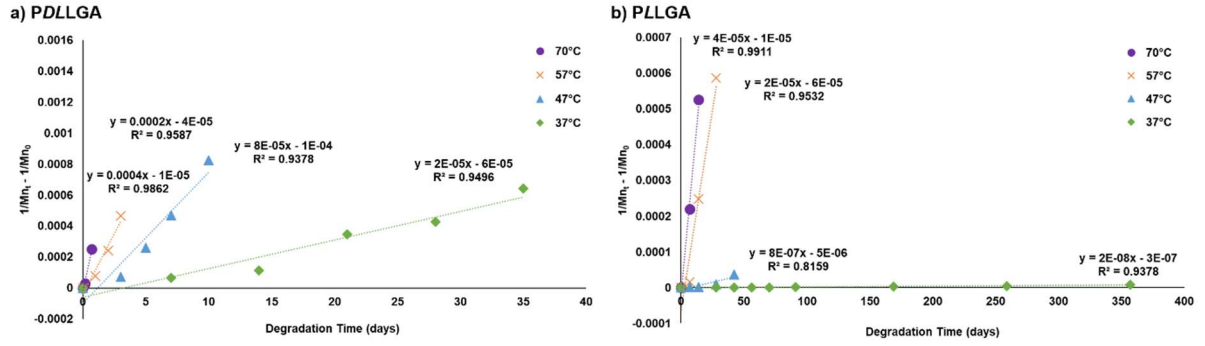

Figure 13. Un-catalysed degradation model for a) PDLLGA and b) PLLGA

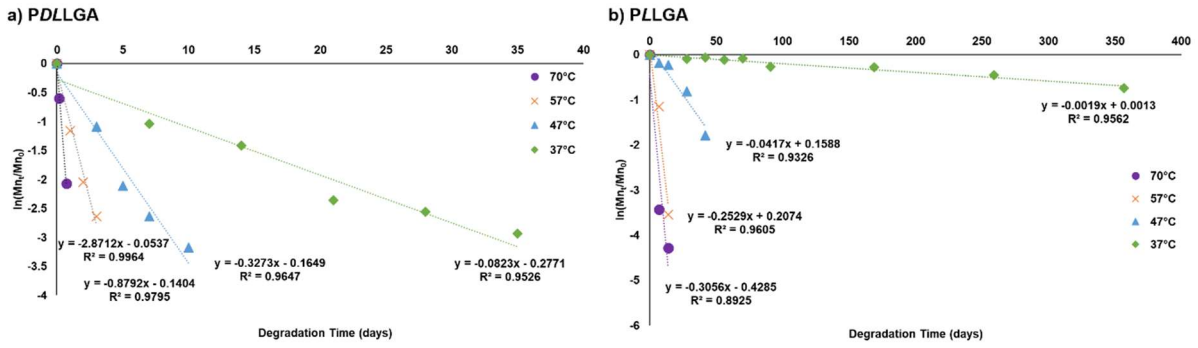

Figure 14. Auto-catalysed degradation model for a) PDLLGA and b) PLLGA

Table 7. Rate constants and correlation coefficients (R^2 value) for the un-catalysed and auto-catalysed models of PDLLGA and PLLGA

Model	*Un-Catalysed*				*Auto-Catalysed*			
Material	**P*DL*LGA**		**P*L*LGA**		**P*DL*LGA**		**P*L*LGA**	
Temperature	k_1	R^2	k_2	R^2	k_3	R^2	k_4	R^2
37°C	2×10^{-5}	0.9496	2×10^{-8}	0.9378	0.0823	0.9526	0.0019	0.9562
47°C	8×10^{-5}	0.9378	8×10^{-7}	0.8159	0.3273	0.9647	0.0417	0.9326
57°C	2×10^{-4}	0.9587	2×10^{-5}	0.9532	0.8792	0.9795	0.2529	0.9605
70°C	4×10^{-4}	0.9862	4×10^{-5}	0.9911	2.8712	0.9964	0.3056	0.8925

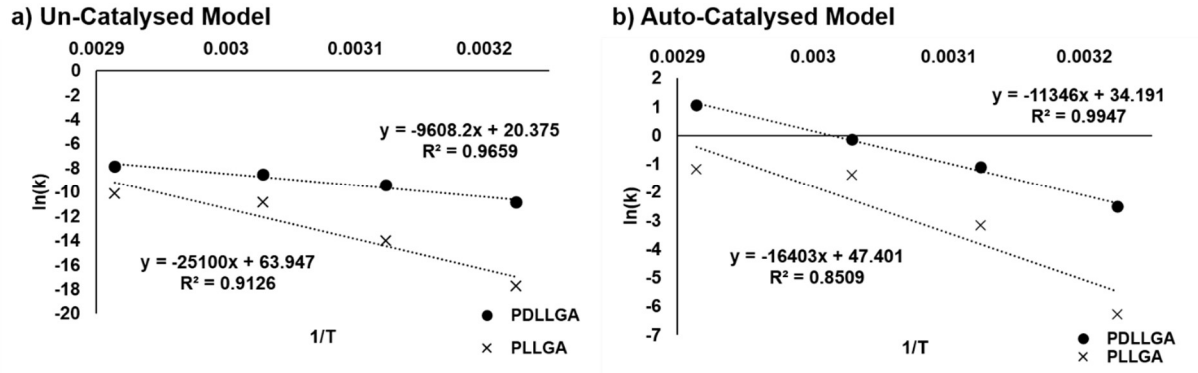

Figure 15. Arrhenius plots of a) Un-catalysed Degradation Model and b) Auto-catalysed Degradation Model for PDLLGA and PLLGA

5.2 Comparison of the Degradation of P*DL*LGA and P*L*LGA

The results of this study suggest that the degradation of P*DL*LGA and P*L*LGA at 47°C, 57°C and 70°C proceed by the same mechanism as for the physiological temperature, 37°C, and the prevailing degradation mechanism is *via* bulk degradation. It is well documented that hydrolysis is initiated

when water diffuses into the polymer and degradation occurs in two distinct phases, where a reduction in molecular weight is observed before any mass loss[2,37]. According to the literature, each polymer in the Poly(lactide-*co*-glycolide) (PLGA) family exhibits different characteristics during bulk degradation, which are due to a number of complex factors, such as polymer morphology, composition and configurational structures, molecular weight, geometry, presence of residual monomers or the degradation media[37,42]. These differences are evident in the results of the present study as there are clear disparities in the morphological changes and degradation rate of P*DL*LGA and P*L*LGA. Figure 1a shows that during the degradation of P*DL*LGA, the sample undergoes significant changes from a solid into a viscous liquid contained by a hard-outer layer, which became thinner during degradation. Alternatively, P*L*LGA maintained its volumetric structure, however, became fragile and disintegrated into a powder on handling (Figure 1b). This phenomenon was also observed by Li *et al.*[43] during the degradation of P*DL*LGA (75:25) and P*L*LGA (75:25); where P*DL*LGA formed a viscous liquid after 21 days at 37°C and P*L*LGA samples formed a white powder after 9 weeks at 37°C.

There are significant differences in the percentage swelling of P*DL*LGA and P*L*LGA. Figure 4 shows that swelling of P*DL*LGA occurs immediately upon immersion in PBS buffer and continues throughout degradation without significant mass loss. A similar trend was observed by Farahani *et al*.[44] when degrading P*DL*LGA (50:50) at 37°C; swelling occurred immediately upon immersion in PBS buffer and continued throughout degradation, reaching a maximum swelling value of 140%. P*DL*LGA is more susceptible to hydrolysis as water readily penetrates the amorphous *D,L* regions. The high rate of water absorption into P*DL*LGA can result in the centre of the polymer degrading more rapidly than the surface. As the molecular weight in the centre of the polymer decreases, by random chain scission, no mass loss occurs initially, as the chains formed by this scission are too large to diffuse out of the polymer matrix. An accumulation of these acidic by-products creates an osmotic concentration difference between the centre of the polymer and the surrounding media, resulting in further water penetration and polymer swelling[2,3,37,45]. In contrast, swelling in P*L*LGA occurred only when mass was lost from the polymer (Figure 5). The more organised crystalline structure of P*L*LGA controls the amount of water uptake into the polymer. As the molecular weight of the P*L*LGA decreases during hydrolysis, the shorter chains become more mobile, making it easier to rearrange into a more crystalline structure[3,46]. Table 4 shows that the crystallinity of P*L*LGA increases during degradation.

The change in pH of the degradation media surrounding the P*DL*LGA and P*L*LGA samples at each temperature (Figure 2) mirrored the changes in mass observed in Figure 3, confirming the release of acidic degradation products from both polymers. This change is important to consider as increasing the acidity of the degradation media catalyses the hydrolysis reaction. Therefore, when the solubility limit of the PBS buffer is reached, the degradation rate of the samples increases and the degradation mechanism is *via* both bulk and surface degradation[3]. Studies on the influence of molecular weight on degradation show that significant erosion of the polymer does not occur until the molecular weight has dropped to a critical level. Once this critical level has been reached, oligomers are small enough to diffuse from the bulk polymer into the degradation media and substantial polymer erosion begins[39,44]. Significant drops in the mass and T*g* were observed (Figures 11 and 12) when the *Mn* dropped below approximately 1150–3600 g/mol in P*DL*LGA and 1200–4400 g/mol in P*L*LGA, suggesting these are the critical values for the specific polymers used in this study.

Residual monomer content is often not reported in publications; however, it is important to consider when analysing the degradation of bioresorbable polymers. The residual monomer present in P*DL*LGA and P*L*LGA can be observed in Figures 8 and 9, in the red boxes A-H, at elution times around

19.3-20.5min. For P*DL*LGA, the residual monomer peak initially has a low refractive index signal and hence a small area under the peak in the chromatogram, in the non-degraded samples, but it increases significantly during degradation, most notably in Figures 8a (box A) and 8b (box B). This suggests that P*DL*LGA is degrading into very short (low molecular weight) chains, which are being retained within the polymer matrix. This contrasts with the relatively small increase in the area under the monomer peak in the P*L*LGA chromatograms, observed in Figure 9, boxes E-H. The biocompatibility of bioresorbable polymers may be affected by the amount of monomer retained within the polymer matrix. The results of this study demonstrate that P*DL*LGA has a higher amount of oligomers and monomers at the later stages of degradation, which are more acidic than P*L*LGA. This is an important factor to consider when examining the *in vitro* or *in vivo* biocompatibility of these polymers. Gleadall[35] suggested that residual monomer content in virgin medical grade bioresorbable polymers should be kept below 2%, to ensure predictable degradation and to prevent the release of high amounts of monomer *in vivo.*

5.3 Determination of the Degradation Mechanism of P*DL*LGA and P*L*LGA

It can be difficult to establish which hydrolysis mechanism is dominant, as the degradation of aliphatic polyesters is complex[47,48]. Mathematical models developed by Anderson[29] and Pitt and Gu[33] were used in this study to model the rate of reduction of molecular weight of P*DL*LGA and P*L*LGA during degradation at 37°C, 47°C, 57°C and 70°C. It is likely that the rate of chain scission leading to a decrease in molecular weight occurs as a result of both un-catalysed and auto-catalysed mechanisms. Only a few studies compare the use of the un-catalysed and auto-catalysed models. Anderson[29,49] found that there was no significant difference between the un-catalysed and auto-catalysed plots of molecular weight versus degradation time for P*L*LA and P*DL*LA. Weiret al.[4] also concluded the same findings as there was no significant difference between the activation energies calculated for P*L*LA using the two models. However, the auto-catalytic model is generally considered to give the best fit of data and is therefore the more commonly used model to analyse degradation when only one model is used[45]. The un-catalysed and auto-catalysed degradation models for P*DL*LGA and P*L*LGA showed a good fit of experimental data, with both models having high R^2 correlation coefficients (Table 7) at each temperature. As the auto-catalysed model has a more consistently high correlation coefficient it is presumed to present a closer approximation of the relationship between molecular weight and degradation time, and any results reported hereafter will reflect this model.

The Arrhenius equation was used to determine the suitability of using increased temperatures to accelerate the degradation of P*DL*LGA and P*L*LGA. Considering the auto-catalysed model for P*DL*LGA, there was a strong fit of data to the Arrhenius plot of $\ln(k_3)$ versus 1/T, with a high R^2 correlation coefficient of 0.9947 and activation energy of 94.3 kJ/mol. For P*L*LGA there was a strong fit of data to the auto-catalysed Arrhenius plot of $\ln(k_4)$ versus 1/T, with an R^2 correlation coefficient of 0.8509 and activation energy of 136.4 kJ/mol. The activation energies of poly (α-hydroxy acids) reported in the literature vary, with values of approximately 83-115 kJ/mol[45]. The activation energy of P*DL*LGA calculated in this study is within this range with PLLGA slightly outside it. Agrawal et al.[23] reported an activation energy of 113.8 kJ/mol for 50:50 PLGA during degradation across a temperature range of 25°C to 80°C. Activation energies of P*DL*LA and P*L*LA microcapsules, determined by Makino et al.[49], were 83.3kJ/mol and 83.7 kJ/mol, respectively, after degradation at 21°C , 37°C and 45°C. The activation energy calculated by Weir et al.[4] for P*L*LA using the auto-catalysed model was 100.5 kJ/mol with an R^2 value of 0.995. The differences in activation energies stated throughout the

literature are most likely due to differences in polymer lactide and glycolide ratios, the geometry of the samples and the testing conditions.

The Arrhenius relationship has been used successfully by several authors to predict the degradation of bioresorbable polymers using increased temperatures[4,26,50]. However, there is some debate in the literature about the validity of using temperatures above the T*g* of a polymer to predict degradation behaviour below the T*g*[23,24]. The properties above and below the T*g* of a polymer can be considerably different. Increasing the temperature above the T*g* increases the internal chain movement, leading to an increase in free volume as Van der Waal forces in amorphous regions are broken. Hydrolysis is initiated as water molecules occupy the free space, resulting in an increase in random chain scission and a faster rate of degradation[4,23]. However, this theory is complicated by the fact that as water enters the molecular structure it acts as a plasticiser, increasing the free volume. This reduces the T*g* as chains are able to move around more easily at a lower temperature[51]. A decrease in T*g* at 37°C, 47°C, 57°C and 70°C is observed in Figure 12 as the molecular weight of P*DL*LGA and P*L*LGA decreases. The results of this study suggest that there is no difference in the degradation mechanism above and below the T*g*. It is, however, important to take into consideration the effect of elevated temperatures on bioresorbable polymers when carrying out accelerated degradation testing.

The degradation of P*DL*LGA and P*L*LGA at elevated temperatures obeyed the Arrhenius relationship and is, therefore, assumed to be a valid method to accelerate their degradation. Based on the findings from this study, 47°C was selected as the optimum temperature to accelerate the degradation of P*DL*LGA and P*L*LGA. Concerns about the validity of the results are also reduced as 47°C is below the T*g* of both P*DL*LGA and P*L*LGA. Hukins et al[27] proposed that increasing the temperature by 10°C roughly doubles the degradation rate of most polymers. In this study, the degradation rate of P*DL*LGA at 47°C is relatively consistent with this finding, with the rate of degradation increasing by x4 for P*DL*LGA. However, it is significantly higher in P*L*LGA with a degradation rate of x21.9 at 47°C.

6 Conclusions

It is paramount that long-term performance of new bioresorbable devices can be demonstrated and compared multilaterally *via* internationally standardised methods. An accelerated degradation methodology has been validated in this study. This allows insight into the likely long-term performance of such materials in a relatively short window of time. It is proposed that 47°C is adopted by the research community when assessing the long-term response of these polymers. However, appropriate testing should be carried out to determine the rate constants when using polymers with different monomer ratios.

A proposed application of this methodology is as a highly effective tool for pre-degrading P*DL*LGA and P*L*LGA bioresorbable polymers prior to evaluation of their long-term *in vitro* inflammatory response. This goes beyond the typically short-term biocompatibility testing that is commonly used to evaluate degradable biomaterials.

Differences observed in the degradation behaviour of the two polymers, suggest that P*L*LGA is more suited for orthopaedic applications due to its degradation behaviour and much lower tendency to swell.

Acknowledgements

Corbion Biomaterials, The Netherlands, is acknowledged for the kind gift of Poly(*D, L*-lactide-co-glycolide) and Poly(*L*-lactide-co-glycolide).

This work has been funded by Department for Economy, Northern Ireland via a PhD Studentship.

References

1. Pina, S. & Ferreira, J. Bioresorbable Plates and Screws for Clinical Applications: A Review. *J. Healthc. Eng.* **3**, 243–260 (2012).

2. Ginjupalli,K., Shavi, G.V. Averineni, R.K., Bhata, M., Udupa, N., Nagaraja Upadhya, P. Poly(α-hydroxy acid) based polymers: A review on material and degradation aspects. *Polym. Degrad. Stab.* **144**, 520–535 (2017).

3. Cameron, R. E. & Kamvari-Moghaddam, A. Synthetic bioresorbable polymers. in *Durability and Reliability of Medical Polymers* 96–118 (2012). doi:10.1016/B978-1-84569-929-1.50005-2

4. Weir NA, Buchanan FJ, Orr JF, Farrar DF, D. G. Degradation of poly-L- lactide. Part 2: increased temperature accelerated degradation. *Proc IME H J Eng Med* **218**, 321–30 (2004).

5. Farrar, D. Bioresorbable Polymers in Orthopaedics. *Biomaterials* **6**, 1–4 (2005).

6. Middleton, J. C. & Tipton, A. J. Synthetic biodegradable polymers as orthopedic devices. *Biomaterials* **21**, 2335–2346 (2000).

7. Tiainen, J., Soini, Y., Törmälä, P., Waris, T. & Ashammakhi, N. Self-reinforced polylactide/polyglycolide 80/20 screws take more than 1 1/2 years to resorb in rabbit cranial bone. *J. Biomed. Mater. Res. - Part B Appl. Biomater.* **70**, 49–55 (2004).

8. Palmer, I., Clarke, S. A. & Buchanan, F. J. Enhanced release of calcium phosphate additives from bioresorbable orthopaedic devices using irradiation technology is non-beneficial in a rabbit model an animal study. *Bone Jt. Res.* **8**, 266–274 (2019).

9. Yang, L., Li, J., Jin, Y., Li, M. & Gu, Z. In vitro enzymatic degradation of the cross-linked poly(ε-caprolactone) implants. *Polym. Degrad. Stab.* **112**, 10–19 (2015).

10. Bourke, H. E. Salmon, L.J., Waller, A., Winalski, C.S., Williams, H.A., Linklater, J.M., Vasanji, A., Roe, J.P., Pinczewski, L.A. Randomized controlled trial of osteoconductive fixation screws for anterior cruciate ligament reconstruction: A comparison of the calaxo and milagro screws. *Arthrosc. - J. Arthrosc. Relat. Surg.* **29**, 74–82 (2013).

11. Song, R. Murphy, M., Li, C., Ting, K., Soo, C., Zheng, Z. Current development of biodegradable polymeric materials for biomedical applications. *Drug Des. Devel. Ther.* **12**, 3117–3145 (2018).

12. Ambrose, C. G. & Clanton, T. O. Bioabsorbable implants: review of clinical experience in orthopedic surgery. *Ann Biomed Eng* **32**, 171–177 (2004).

13. Konan, S. & Haddad, F. S. A clinical review of bioabsorbable interference screws and their adverse effects in anterior cruciate ligament reconstruction surgery. *Knee* **16**, 6–13 (2009).

14. Jong, W. H. De, Bergsma, J. E., Robinson, J. E. & Bos, R. R. M. Tissue response to partially in vitro predegraded poly- L -lactide implants. *Biomaterials* **26**, 1781–1791 (2005).

15. Böstman, O. M. & Pihlajamäki, H. K. Late Foreign-Body Reaction to an intraosseuous bioabsorbable polylactic acid screw. *J. Bone Jt. Surg.* **80**-**A**, 1791–1794 (1998).

16. Athanasiou, K. A., Niederauer, G. G. & Agrawal, C. M. Sterilization, toxicity, biocompatibility and clinical applications of polylactic acid / polyglycolic acid copolymers. *Biomaterials* **17**, (1996).

17. Walsh, W. R., Cotton, N.J., Stephens, P., Brunelle, J.E., Langdown, A., Auld, J., Vizesi, F., Bruce, W. Comparison of Poly-L-Lactide and Polylactide Carbonate Interference Screws in an Ovine Anterior Cruciate Ligament Reconstruction Model. *Arthrosc. - J. Arthrosc. Relat. Surg.* **23**, 757–765 (2007).

18. Konan, S. & Haddad, F. S. The unpredictable material properties of bioabsorbable PLC interference screws and their adverse effects in ACL reconstruction surgery. *Knee Surgery, Sport. Traumatol. Arthrosc.* **17**, 293–297 (2009).

19. Cox, C. L. Spindler, K.P., Leonard, J.P., Morris, B.J., Dunn, W.R., Reinke, E.K. Do Newer-Generation Bioabsorbable Screws Become Incorporated into Bone at Two Years After ACL Reconstruction with Patellar Tendon Graft? *J. Bone Jt. Surg.* **96**, 244–250 (2014).

20. Cox, C. L., Homlar, K. C., Carey, J. L. & Spindler, K. P. CALAXO osteoconductive interference screw: the value of postmarket surveillance. *J. Surg. Orthop. Adv.* **19**, 121–124 (2010).

21. George Barnes. *REGENESORB Absorbable Biocomposite Material*. (2013).

22. Barber, F. A., Dockery, W. D. & Hrnack, S. A. Long-term degradation of a poly-lactide co-glycolide/β-tricalcium phosphate biocomposite interference screw. *Arthrosc. - J. Arthrosc. Relat. Surg.* **27**, 637–643 (2011).

23. Agrawal, C., Huang, D., Schmitz, J. P. & Athanasiou, K. A. Elevated Temperature Degradation of a 50:50 Copolymer of PLA-PGA. *Tissue Eng.* **3**, (1997).

24. Lyu, S., Schley, J., Loy, B., Lind, D., Hobot, C., Sparer, R., and Untereker, D. Kinetics and time-temperature equivalence of polymer degradation. *Biomacromolecules* **8**, 2301–2310 (2007).

25. Zolnik, B. S., Leary, P. E. & Burgess, D. J. Elevated temperature accelerated release testing of PLGA microspheres. *J. Control. Release* **112**, 293–300 (2006).

26. D'Souza, S. S., Faraj, J. A. & DeLuca, P. P. A model-dependent approach to correlate accelerated with real-time release from biodegradable microspheres. *AAPS PharmSciTech* **6**, E553-64 (2005).

27. Hukins, D. W. L., Mahomed, A. & Kukureka, S. N. Accelerated aging for testing polymeric biomaterials and medical devices. *Med. Eng. Phys.* **30**, 1270–1274 (2008).

28. Tsuji, H. & Ikada, Y. Physical properties of polylactides. *Curr Trends Polym Sci* **4**, 27 (1999).

29. Anderson, J. M. Perspectives on the in vivo responses of biodegradable polymers. *Biomed. Appl. Synth. Biodegrad. Polym.* 223–233 (1995).

30. Han, X., Pan, J., Buchanan, F., Weir, N. & Farrar, D. Analysis of degradation data of poly(l-lactide-co-l,d-lactide) and poly(l-lactide) obtained at elevated and physiological temperatures using mathematical models. *Acta Biomater.* **6**, 3882–3889 (2010).

31. Farrar, D. F. & Gillson, R. K. Hydrolytic degradation of polyglyconate B: The relationship between degradation time, strength and molecular weight. *Biomaterials* **23**, 3905–3912 (2002).

32. Vroman, I. & Tighzert, L. *Biodegradable polymers*. *Materials* **2**, (2009).

33. Pitt, C. & Gu, Z. Modification of the rates of chain cleavage of poly(ϵ-caprolactone) and related polyesters in the solid state. *J. Control. Release* **4**, 298–292 (1987).

34. Grizzi, I., Garreau, H., Li, S. & Vert, M. Hydrolytic degradation of devices based on poly(dl-lactic acid) size-dependence. *Biomaterials* **16**, 305–311 (1995).

35. Gleadall, A., Pan, J., Kruft, M. A. & Kellomäki, M. Degradation mechanisms of bioresorbable polyesters. Part 2. Effects of initial molecular weight and residual monomer. *Acta Biomater.* **10**, 2233–2240 (2014).

36. Hakkarainen, M., Albertsson, A. C. & Karlsson, S. Weight losses and molecular weight changes correlated with the evolution of hydroxyacids in simulated in vivo degradation of homo- and copolymers of PLA and PGA. *Polym. Degrad. Stab.* **52**, 283–291 (1996).

37. Li, S. Hydrolytic degradation characteristics of aliphatic polyesters derived from lactic and glycolic acids. *J Biomed Mater Res (Appl Biomater)* **48**, 342–353 (1998).

38. Park, P. I. P. & Jonnalagadda, S. Predictors of glass transition in the biodegradable polylactide and poly-lactide-co-glycolide polymers. *J. Appl. Polym. Sci.* **100**, 1983–1987 (2006).

39. Braunecker, J., Baba, M., Milroy, G. E. & Cameron, R. E. The effects of molecular weight and porosity on the degradation and drug release from polyglycolide. *Int. J. Pharm.* **282**, 19–34 (2004).

40. Park, T. G. Degradation of poly(lactic-co-glycolic acid) microspheres: effect of copolymer composition. *Biomaterials* **16**, 1123–1130 (1995).

41. J. E. BERGSMA, F. R. ROZEMA, R. R. M. BOS, G. B. In vitro predegradation at elevated temperatures of poly (lactide). *J. Mater. Sci. Mater. Med.* **6**, 642–646 (1995).

42. Li, S. & Vert, M. Biodegradation of Aliphatic Polyesters. in *Degradable Polymers: Principles and Applications* (Springer, Dordrecht, 1995). doi:10.1007/978-94-017-1217-0_5

43. Li, S. M., Garreau, H. & Vert, M. Structure-property relationships in the case of the degradation of massive poly(α-hydroxy acids) in aqueous media - Part 2 Degradation of lactide-glycolide copolymers: PLA37.5GA25 and PLA75GA25. *J. Mater. Sci. Mater. Med.* **1**, 131–139 (1990).

44. Darestabi Farahani, T., Akbar Entezami, A., Mobedi, H. & Abtahi, M. Degradation of Poly(D,L-lactide-co-glycolide) 50:50 Implant in Aqueous Medium. *Iran. Polym. J.* **14**, 753–763 (2005).

45. Farrar, D. Modelling of the degradation process for bioresorbable polymers. *Degrad. rate bioresorbable Mater.* 183–206 (2008). doi:10.1533/9781845695033.3.183

46. Chan, J. C. Y., Burugapalli, K., Kelly, J. L. & Pandit, A. S. 12 – Influence of clinical application on bioresorbability: Host response. in *Degradation Rate of Bioresorbable Materials* 267–318 (2008). doi:10.1533/9781845695033.5.267

47. Gleadall, A., Pan, J., Kruft, M. A. & Kellomäki, M. Degradation mechanisms of bioresorbable polyesters. Part 1. Effects of random scission, end scission and autocatalysis. *Acta Biomater.* **10**, 2223–2232 (2014).

48. Gleadall, A. MODELLING DEGRADATION OF BIODEGRADABLE Thesis submitted for the degree of Doctor of Philosophy At the University of Leicester by Andrew Colin Gleadall (MEng) Department of Engineering University of Leicester. *Transition* (2015).

49. Makino, K., Arakawa, M. & Tamotsu, K. Preparation and in vitro Degradation Properties of Polylactide Microcapsules. *Biol. Pharm. Bull.* **33**, 1195–1201 (1985).

50. Burkley, D., Zhou, J., Chen, G., Burkley, D., Xu, Y., Jamiolkowski, D., Barbolt, T. Effect of load and temperature on in vitro degradation of poly(glycolide-co-l-lactide) multifilament braids. *Biomaterials* **26**, 4327–4336 (2004).

51. Jadhav, N., Gaikwad, V., Nair, K. & Kadam, H. Glass transition temperature: Basics and application in pharmaceutical sector. *Asian J. Pharm.* **3**, 82 (2009).